

BASIC CHARACTERISATION OF OIL PALM SHELL
AS CONSTRUCTED WETLAND MEDIA AND THE
EFFECT OF BIOFILM FORMATION ON ITS
ADSORPTION OF COPPER (II)

HARRY CHONG LYE HIN

UNIVERSITI SAINS MALAYSIA

2008

**BASIC CHARACTERISATION OF OIL PALM SHELL AS CONSTRUCTED
WETLAND MEDIA AND THE EFFECT OF BIOFILM FORMATION
ON ITS ADSORPTION OF COPPER (II)**

by

HARRY CHONG LYE HIN

**Thesis submitted in fulfillment of the
requirements for the degree of
Doctor of Philosophy**

April 2008

ACKNOWLEDGEMENTS

It gives me much pleasure to thank the following marvellous God's creations:

Associate Professor Dr. Ahmad Md. Noor (supervisor) and Professor Dr. Lim Poh Eng (co-supervisor) for their guidance and unfailing interest, which transformed an interesting research project into a thoroughly enjoyable one.

The Malaysian government via the Ministry of Science, Technology and Environment (MoSTE: IRPA grant 305/PKIMIA/610810), Universiti Sains Malaysia (USM) and Universiti Malaysia Sabah (UMS) that provided the much needed financial assistances.

The Microscopy Unit (School of Biological Sciences, USM) and Analytical Services Unit (School of Chemical Sciences, USM) for their material and technical assistances.

Tee Heng Chong who has spiced up the research project by just simply being what he is, the most kind hearted and a brilliant post graduate student that I will always remember.

Pedy Artsanti who has hand in hand set up the lab from scrap with me. A friend that I will never forget for her will power.

Associate Professor Dr. Seng Chye Eng (USM) for his assistance and advices during the research.

Other fellow research students, in particular Flora Tan, Oo Chuan Wei, Yap Chin Yean, Adeline Poh, Yashoda and Vanitha for their assistances and encouragements which they may not realise it.

The staff of School of Chemical Sciences (USM) and the many others who have helped directly and indirectly in very unique ways.

Both my parents who have been counting the days with the hope I will graduate as soon as possible.

I must thank my wife, Daisy Jombing, for her unconditional constant understanding, encouragement and patience for the days and nights when I was writing this thesis.

CONTENTS

Title page	i
Acknowledgements	ii
Contents	iii
List of Tables	viii
List of Figures	xi
List of Plates	xviii
List of Symbols	xxi
List of Abbreviations	xxiii
List of Appendixes	xxvi
Abstrak (Malay Language Translation of Abstract)	xxvii
Abstract	xxviii
Chapter 1 Introduction	
1.1 The Birth of Idea	1
1.2 Constructed Wetland	3
1.2.1 Definition	3
1.2.2 Basic components	4
1.2.3 Design	5
1.2.4 General applications	6
1.2.5 Treatment of heavy metal	7
1.3 Malaysia Oil Palm Scenario	9
1.3.1 Sabah oil palm sector	11
1.4 Copper	11
1.4.1 Mamut copper mine	12
1.5 Biofilm	14
1.5.1 Definition	14
1.5.2 Formation	14
1.5.3 Conceptual models	16
1.5.4 Extracellular polymeric substances	16
1.5.5 Persistency	17
1.5.6 Notes on biofilm-heavy metal	18
1.6 Research Objectives	19
1.6.1 Further descriptions on research objectives	21
Chapter 2 Materials and Methods	
2.1 Reagents	22
2.2 Sewage	23
2.3 Preparation of Media	23
2.3.1 Preparation of pea gravel	24

2.3.2	Preparation of oil palm shell and mesocarp fibre	25
2.3.3	Preparation of coconut shell and mesocarp fibre	26
2.3.4	Preparation of rice hull	26
2.3.5	Preparation of sugarcane fibre	27
2.3.6	Preparation of coarse sand, fine sand and wood shave	27
2.3.7	Preparation of granular activated carbon and zeolite	28
2.3.8	Precautions on media preparation	28
2.4	Preparation of <i>Typha angustifolia</i>	29
2.5	Preparation of Samples for Scanning Electron Microscopy and Energy Dispersive X-ray Spectroscopy	32
2.6	Instrumental Analyses	33
2.6.1	Macroscopy	33
2.6.2	pH determination	34
2.6.3	Porosimetry	34
2.6.4	Scanning electron microscopy and energy dispersive x-ray spectroscopy	35
2.6.5	Elemental analysis	35
2.6.6	Thermogravimetry analysis	35
2.6.7	Fourier transformed infra-red spectroscopy	36
2.6.8	Flame atomic absorption spectrometry	36
2.7	Preliminary Study on Various Media	36
2.7.1	Comparative adsorption study	36
2.7.2	Characterisation study	37
2.8	Microcosms Experiment	37
2.8.1	Preparation of microcosms	37
2.8.2	Monitoring the height and shoots of <i>Typha angustifolia</i> in microcosms	41
2.8.3	Monitoring the biomass gain of <i>Typha angustifolia</i> in microcosms	41
2.8.4	Monitoring the pH of microcosms and other qualitative properties	43
2.8.5	Morphological study on the experimented media	43
2.8.6	Adsorption isotherms of the <i>Typha angustifolia</i> biomass	44
2.9	Mesocosm Experiment	44
2.9.1	Preparation of mesocosm	44
2.9.2	Monitoring the growth of <i>Typha angustifolia</i> in mesocosm	48
2.9.3	Monitoring the pH of mesocosm	49
2.9.4	Morphological study on media from different depths	49
2.9.5	Adsorption isotherms of the media from different depths	50
2.10	Study on the Growth of Biofilm in Isolated Systems	51
2.10.1	Preparation of the liquid media	51
2.10.2	Sterilisation	51
2.10.3	Conditions of experiment	51
2.10.4	Macroscopy documentation	52
2.10.5	Microscopy documentation	52
2.11	Adsorption Study on the Selected Media	53
2.11.1	Batch experiments	53
2.11.2	Column experiments	54
2.11.2a	Adsorption study	54
2.11.2b	Regeneration study	56
2.11.2c	Distribution of Cu (II) on the utilised media	56
2.12	Study on the Selected Biofilmed Media	56
2.12.1	Preparation of biofilmed media	56
2.12.2	Characterisation study on the selected biofilmed media	57

	2.12.3 Batch adsorption experiments	57
	2.12.4 Column adsorption experiments	58
Chapter 3	Results	
3.1	Preliminary Study on Various Media	59
3.1.1	The prepared media	59
3.1.2	Comparative heavy metal removal efficiency	62
3.1.3	Characterisation of some media	63
	3.1.3a pH	63
	3.1.3b Surface area and pore distribution	64
	3.1.3c Surface morphology	67
	3.1.3d C, H and N contents	70
	3.1.3e Thermogravimetry result	71
	3.1.3f FT-IR spectrum	72
3.2	Microcosms Experiment	73
3.2.1	Height growth	73
3.2.2	Shoot generation	76
3.2.3	Biomass gain	78
	3.2.3a Above-ground plant biomass	78
	3.2.3b Below-ground plant biomass	79
3.2.4	pH of effluents	80
3.2.5	Other qualitative observations	81
3.2.6	Imagery of the experimented media	84
3.2.7	Adsorption isotherm of the dried <i>Typha angustifolia</i> biomass	87
3.3	Mesocosm Experiment	89
3.3.1	Height growth	89
3.3.2	Shoot generation	93
3.3.3	pH of the mesocosm fluid	94
3.3.4	Morphology of the media “incubated” at different depths	94
3.3.5	Adsorption isotherm of the media “incubated” at different depths	96
3.4	Growth of biofilm in isolated systems	97
3.5	Adsorption Study on the Media without Biofilm Formation	98
3.5.1	Batch experiments	98
	3.5.1a Effect of pH_i	98
	3.5.1b Effect of contact time	100
	3.5.1c Effect of particle size	102
	3.5.1d Effect of dosage	103
	3.5.1e Effect of particle size and contact time	105
	3.5.1f Effect of dosage and contact time	106
	3.5.1g Effect of initial concentration and contact time	107
	3.5.1h Adsorption isotherm	108
3.5.2	Column experiments	110
	3.5.2a Effect of flow rate	110
	3.5.2b Effect of bed depth	111
	3.5.2c Effect of influent concentration	112
	3.5.2d Adsorption-desorption and reutilisation study	113
	3.5.2e Distribution of Cu (II) on the surface of the used OPS	114
3.6	Study on the Biofilmed Media	116
3.6.1	Physico-chemistry characteristics	116
3.6.2	Batch experiments	120

	3.6.2a Comparative heavy metal removal efficiency	120
	3.6.2b Effect of pH _i	120
	3.6.2c Effect of contact time	121
	3.6.2d Effect of dosage	122
	3.6.2e Effect of initial concentration and contact time	123
	3.6.2f Adsorption isotherm	124
3.6.3	Column experiments	125
	3.6.3a Effect of flow rate	125
	3.6.3b Effect of bed depth	126
	3.6.3c Effect of influent concentration	127
	3.6.3d Adsorption-desorption and reutilisation study	128
	3.6.3e Distribution of Cu (II) on the surface of the used OPSB	129
Chapter 4	Discussion of Results	
4.1	Experimental Constructed Wetland System Designs	131
	4.1.1 pH of waterbody	132
	4.1.2 Height of <i>Typha angustifolia</i> plantlets	133
	4.1.3 Shoots density	134
	4.1.4 Preliminary conclusion	136
4.2	Experimental Constructed Wetland Media	136
	4.2.1 pH of waterbody	137
	4.2.2 Plants height	139
	4.2.3 Shoots density	140
	4.2.4 Dry plant biomass gain	143
	4.2.5 OPS as a constructed wetland media	143
4.3	Removal of Cu (II), Cd (II), Zn (II) and Pb (II) by Some Media	144
4.4	Formation of Biofilm	145
4.5	Effect of Biofilm Formation on the Physico-chemistry Properties of Some Media	146
	4.5.1 Morphology	146
	4.5.2 pH	152
	4.5.3 Surface area and pore distribution	153
	4.5.4 C, H and N contents	156
	4.5.5 Thermogravimetry results	158
	4.5.6 FT-IR spectra	158
	4.5.7 The propose barrier effect on the adsorption of Cu (II)	159
4.6	The Effect of Biofilm Formation on the Removal of Cu (II) in Batch Experiments	163
	4.6.1 Effect of various media	163
	4.6.2 Effect of various pH _i	164
	4.6.3 Effect of contact time and initial concentration	166
	4.6.4 Effect of dosage	169
	4.6.5 Adsorption isotherms	171
	4.6.5a Langmuir isotherm	172
	4.6.5b Freundlich isotherm	175
	4.6.6 Adsorption kinetics	177
	4.6.6a External mass transfer diffusion model / Boundary layer effect	178
	4.6.6b Intraparticle diffusion	183
	4.6.6c Pseudo-second order equation	186
4.7	The Effect of Biofilm Formation on the Adsorption of Cu (II) in Column Experiments	190

4.7.1	Effect of flow rate	190
4.7.2	Effect of bed depth	192
4.7.3	Effect of influent concentration	195
4.7.4	Adsorption, recovery and regenerated adsorption of the media	197
4.7.5	Copper distribution	198
4.8	Theoretical Maximum Adsorption of Cu (II) in a Constructed Wetland	199
Chapter 5	Conclusion and Suggestions	
5.1	Growth of <i>Typha angustifolia</i> in OPS-based Experimental Constructed Wetland Unit	201
5.2	Biofilm Formation on OPS	201
5.3	Effects of Biofilm Formation on OPS on the Adsorption of Cu (II)	202
5.4	Environmental Considerations	205
5.5	Recommendation for Further Research	206
References		208
Appendixes		222
Publication List		294

LIST OF TABLES

Table 1.1	Examples of various pollutants treated utilising constructed wetland wastewater treatment system	7
Table 2.1	Chemicals used in this study	22
Table 2.2	Categorisation of media	24
Table 2.3	Media and void pores data of each microcosm	39
Table 2.4	Plantlet specification as on Day 0 and Day 55 prior to planting	40
Table 2.5	Maximum length of each plantlet in mesocosm on Day 0	47
Table 2.6	Conditions of experiment in studying the growth of biofilm in isolated systems	52
Table 2.7	Condition of each batch experiment	54
Table 2.8	Condition of each column experiment	55
Table 2.8	Condition of each batch adsorption experiment	58
Table 3.1	The pH of various media	64
Table 3.2	Porosimetry results of the analysed media samples	65
Table 3.3	C, H and N contents of the analysed media samples	71
Table 3.4	Simplified interpretation of the OPS FT-IR spectrum	73
Table 3.5	Above-ground plant biomass gain throughout the experiment	79
Table 3.6	Constants of the Langmuir and Freundlich models for the adsorption of Cu (II) by dried <i>Typha angustifolia</i> leaves and roots	88
Table 3.7	Constants of the Langmuir and Freundlich models for Cu (II) adsorption by OPSB-Top and OPSB-Bottom	97
Table 3.8	Results of biofilm formation in isolated systems	98
Table 3.9	Minimum contact time and removal efficiency of the batch systems at equilibrium	101
Table 3.10	Heavy metal uptake by OPS of various particle sizes	103
Table 3.11	Removal efficiency of Cu (II) by OPS and OPF at various dosages	104

Table 3.12	Constants of the Langmuir and Freundlich models for Cu (II), Cd (II), Zn (II) and Pb (II) adsorption by G, OPS, OPF, GAC and Zeo	110
Table 3.13	Removal efficiency of Cu (II) treated in the OPS-packed column of 10 cm bed depth at various flow rates	111
Table 3.14	Removal efficiency of Cu (II) treated in the OPS-packed column of various bed depths at the flow rate of 10 mL/min	112
Table 3.15	Removal efficiency of Cu (II) of various C_{in} treated in the OPS-packed column (10 cm bed depth) at the flow rate of 10 mL/min	113
Table 3.16	SEM-EDX results for the Cu (II) laden OPS sample	115
Table 3.17	pH of the biofilmed media	116
Table 3.18	Porosimetry results for the GB and OPSB samples	116
Table 3.19	C, H and N contents of the OPSB and OPFB samples	117
Table 3.20	Simplified interpretation of the OPSB FT-IR spectrum	119
Table 3.21	Constants of the Langmuir and Freundlich models for the adsorption of Cu (II) by GB, OPSB, OPFB, GACB and ZeoB	125
Table 3.22	Removal efficiency of Cu (II) treated in the OPSB-packed column of 10 cm bed depth at various flow rates	126
Table 3.23	Removal efficiency of Cu (II) treated in the OPSB-packed column of various bed depths at the flow rate of 10 mL/min	127
Table 3.24	Removal efficiency of Cu (II) of various C_{in} treated in the OPSB-packed column (10 cm bed depth) at the flow rate of 10 mL/min	127
Table 3.25	SEM-EDX results for the Cu (II) laden OPSB sample	129
Table 4.1	Mathematical description on shoots density as a function of time	136
Table 4.2	Shortlisted media and their roles	137
Table 4.3	Mathematical expression of shoots density in various media-based microcosms	142
Table 4.4	Rate of dry plant biomass gain in each microcosm	143
Table 4.5	Comparative porosimetry results for the G and OPS media without and with biofilm formation	154
Table 4.6	Comparative C, H and N contents of the G- and OPS-based media samples	156
Table 4.7	Comparative thermogravimetry results of the OPS and OPSB samples	158

Table 4.8	Removal of Cu (II) by selected media without and with biofilm formation	163
Table 4.9	Langmuir constants for the adsorption of Cu (II) by selected media without and with biofilm formation	173
Table 4.10	Comparative adsorption capacities of the experimented media and some low-cost sorbents for the adsorption of Cu (II)	174
Table 4.11	Freundlich constants for the adsorption of Cu (II) by selected media without and with biofilm formation	176
Table 4.12	Pseudo-second order rate constants for the Cu (II) adsorption by G, GB, OPS, OPSB, OPF and OPFB	188
Table 4.13	Percentage of removal of the Cu (II) treated in the OPS- and OPSB-packed columns at various flow rates	192
Table 4.14	Utilised capacity of the OPS- and OPSB-packed columns employing different bed depths for the adsorption of Cu (II)	193
Table 4.15	Adsorption performance of the OPS- and OPSB-packed columns receiving Cu (II) of various C_{in}	196
Table 4.16	Recovery of Cu (II) from the utilised OPS- and OPSB-packed columns utilising 0.1 M HNO_3	198
Table 4.17	Comparative SEM-EDX area scan results of the OPS and OPSB experimented with Cu (II) in the column experiments	199
Table 4.18	Theoretical maximum Cu (II) adsorption in each microcosm	200

LIST OF FIGURES

Figure 1.1	Malaysia's palm oil highlights	10
Figure 1.2	Processes governing biofilm formation	15
Figure 1.3	Diagrammatic representation of the structure of the hypothetical bacterial biofilm drawn from confocal scanning laser microscopy (CSLM) examination of a large number of mono- and mixed-species biofilms. The discrete microcolonies of microorganisms are surrounded by a network of interstitial voids filled with water. The arrows indicate convective flow within the water channels	16
Figure 1.4	Proposed model for dominating intermolecular interactions which contribute to mechanical stability in a biofilm. Five different phenomena are considered. 1 = repulsive electrostatic interactions between ionic residues; 2 = attractive electrostatic forces, typically in the presence of divalent cations; 3 = hydrogen bonds; 4 = other electrostatic interactions, e.g. between dipoles; 5 = London (dispersion) interactions	17
Figure 2.1	The pH of the heavy metal solutions at various concentrations	23
Figure 2.2	Schematic drawing showing the front and side views of the microcosm tank	38
Figure 2.3	Top view of the microcosm	40
Figure 2.4	Top view and side cross section of the mesocosm (plantlets are not shown in the side cross section drawing)	45
Figure 2.5	Front cross section and rear view of the mesocosm	46
Figure 2.6	Distribution of zones, plantlets and sampling ports in the mesocosm	46
Figure 2.7	Hydraulic flow path of the entire mesocosm system	47
Figure 2.8	Details on media "incubation" in the mesocosm for morphological study	49
Figure 2.9	Details on media "incubation" in the mesocosm for adsorption isotherm study	50
Figure 2.10	General flow process of the batch experiments	53
Figure 2.11	Experimental set up of the column experiment	55
Figure 2.12	Sampling zone of the media in microcosm	57
Figure 3.1	Comparative heavy metal removals by various media	63

Figure 3.2	Comparative average pore diameter of the analysed media samples	65
Figure 3.3	Adsorption pore distribution of the G, OPS and CS samples	66
Figure 3.4	Adsorption pore distribution of the OPF, CF and WS samples	66
Figure 3.5	Adsorption pore distribution of the GAC and Zeo samples	67
Figure 3.6	Thermogram of the OPS sample (30 – 900 °C)	72
Figure 3.7	FT-IR spectrum of the OPS sample	73
Figure 3.8	Growth of <i>Typha angustifolia</i> in various media prior to the first harvest	74
Figure 3.9	Growth of <i>Typha angustifolia</i> in various media in between the first and second harvest	75
Figure 3.10	Growth of <i>Typha angustifolia</i> in various media in between the second and third harvest	76
Figure 3.11	<i>Typha angustifolia</i> shoot generation in various media prior to the first harvest	77
Figure 3.12	<i>Typha angustifolia</i> shoot generation in various media in between the first and second harvest	77
Figure 3.13	<i>Typha angustifolia</i> shoot generation in various media in between the second and third harvest	78
Figure 3.14	Dry below-ground plant biomass gain at the end of the experiment	80
Figure 3.15	The pH changes in the microcosms (Days 5 – 180)	80
Figure 3.16	Isotherms of the Cu (II) adsorption by dried <i>Typha angustifolia</i> leaves and roots	88
Figure 3.17	<i>Typha angustifolia</i> height growth in the I row of the mesocosm	89
Figure 3.18	<i>Typha angustifolia</i> height growth in the M row of the mesocosm	90
Figure 3.19	<i>Typha angustifolia</i> height growth in the O row of the mesocosm	90
Figure 3.20	<i>Typha angustifolia</i> height growth in the left- and right-zones of the mesocosm	91
Figure 3.21	<i>Typha angustifolia</i> height growth in the inlet-, middle- and outlet-zones of the mesocosm	92
Figure 3.22	Shoot generation in each zone of the mesocosm	93

Figure 3.23	Overall shoot generation in the mesocosm	93
Figure 3.24	The pH changes in the mesocosm (Days 28 – 145)	94
Figure 3.25	Isotherms of the Cu (II) adsorption by OPSB-Top and OPSB-Bottom	97
Figure 3.26	Adsorption of Cu (II) by G, OPS and OPF at various pH _i	98
Figure 3.27	Adsorption of Cd (II) by G, OPS and OPF at various pH _i	99
Figure 3.28	Adsorption of Zn (II) by G, OPS and OPF at various pH _i	99
Figure 3.29	Adsorption of Pb (II) by G, OPS and OPF at various pH _i	100
Figure 3.30	Effect of contact time on the adsorption of Cu (II)	101
Figure 3.31	Effect of contact time on the adsorption of Cd (II)	101
Figure 3.32	Effect of contact time on the adsorption of Zn (II)	102
Figure 3.33	Effect of contact time on the adsorption of Pb (II)	102
Figure 3.34	Effect of OPS particle size on the adsorption of some bivalent metals	103
Figure 3.35	Effect of OPS and OPF dosages on the adsorption of Cu (II)	104
Figure 3.36	Effect of OPF dosage on the adsorption of some bivalent metals	105
Figure 3.37	Effect of OPS particle size and contact time on the adsorption of Cu (II)	106
Figure 3.38	Effect of OPF dosage and contact time on the adsorption of Pb (II)	107
Figure 3.39	Effect of C _o and contact time on the adsorption of Cu (II) by OPS	107
Figure 3.40	Isotherms of the Cu (II) adsorption by G, OPS, OPF, GAC and Zeo	108
Figure 3.41	Isotherms of the Cd (II) adsorption by G, OPS, OPF, GAC and Zeo	108
Figure 3.42	Isotherms of the Zn (II) adsorption by G, OPS, OPF, GAC and Zeo	109
Figure 3.43	Isotherms of the Pb (II) adsorption by G, OPS, OPF, GAC and Zeo	109
Figure 3.44	Break through curves of Cu (II) treated in the OPS-packed column of 10 cm bed depth at various flow rates	111

Figure 3.45	Break through curves of Cu (II) treated in the OPS-packed column of various bed depths at the flow rate of 10 mL/min	112
Figure 3.46	Break through curves of Cu (II) of various C_{in} treated in the OPS-packed column (10 cm bed depth) at the flow rate of 10 mL/min	113
Figure 3.47	The utilised capacity of the OPS-packed column during the adsorption-desorption and reutilisation experiment	114
Figure 3.48	The elution process of the Cu (II) loaded OPS-packed column utilising 0.1 M HNO_3	114
Figure 3.49	Adsorption pore distribution of the GB and OPSB samples	117
Figure 3.50	Thermogram of the OPSB sample (30 – 900 °C)	118
Figure 3.51	FT-IR spectrum of the OPSB sample	119
Figure 3.52	Comparative Cu (II) removal by various biofilmed media	120
Figure 3.53	Removal of Cu (II) by GB, OPSB and OPFB at various pH_i	121
Figure 3.54	Effect of contact time on the adsorption of Cu (II) by GB, OPSB and OPFB	121
Figure 3.55	Effect of OPSB and OPFB dosages on the adsorption of Cu (II)	122
Figure 3.56	Uptake of Cu (II) by various dosages of OPSB and OPFB	123
Figure 3.57	Effect of C_o and contact time on the uptake of Cu (II) by OPSB	123
Figure 3.58	Isotherms of the Cu (II) adsorption by GB, OPSB, OPFB, GACB and ZeoB	124
Figure 3.59	Break through curves of Cu (II) treated in the OPSB-packed column of 10 cm bed depth at various flow rates	125
Figure 3.60	Break through curves of Cu (II) treated in the OPSB-packed column of various bed depths at the flow rate of 10 mL/min	126
Figure 3.61	Break through curves of Cu (II) of various C_{in} treated in the OPSB-packed column (10 cm bed depth) at the flow rate of 10 mL/min	127
Figure 3.62	The utilised capacity of the OPSB-packed column during the adsorption-desorption and reutilisation experiment	128
Figure 3.63	Elution process of the Cu (II) loaded OPSB-packed column utilising 0.1 M HNO_3	129
Figure 4.1	Comparative pH of the waterbody in the microcosm and mesocosm (Days 30 – 145)	133

Figure 4.2	Comparative height growth of the plantlets in the microcosm and mesocosm (Days 0 – 90)	134
Figure 4.3	Comparative shoots density growth in the microcosm and mesocosm	134
Figure 4.4	Linearised growth in shoots density of the G-based microcosm	135
Figure 4.5	Linearised growth in shoots density of the mesocosm	135
Figure 4.6	Cultural pH requirement and pH changes in each microcosm	138
Figure 4.7	Plants height in the microcosms (Days 0 – 500)	139
Figure 4.8	Linearised growth in shoots density of the OPS-based microcosm	140
Figure 4.9	Linearised growth in shoots density of the OPF-based microcosm	141
Figure 4.10	Linearised growth in shoots density of the GAC-based microcosm	141
Figure 4.11	Linearised growth in shoots density of the Zeo-based microcosm	141
Figure 4.12	Effect of biofilm formation on pH of the media	153
Figure 4.13	Comparative adsorption pore distributions of the G and GB samples	154
Figure 4.14	Comparative adsorption pore distributions of the OPS and OPSB samples	155
Figure 4.15	Comparative FT-IR spectra of the OPS and OPSB samples	159
Figure 4.16	Adsorption of Cu^{2+} ions onto media	160
Figure 4.17	Adsorption of Cu^{2+} ions onto suspended biofilm	160
Figure 4.18	Equilibrated adsorption of Cu^{2+} ions onto suspended biofilm and media	161
Figure 4.19	Adsorption of Cu^{2+} ions onto biofilmed media	162
Figure 4.20	Removal of Cu (II) by selected media without and with biofilm formation	163
Figure 4.21	Adsorption of Cu (II) on the G and GB at various pH_i	165
Figure 4.22	Adsorption of Cu (II) on the OPS and OPSB at various pH_i	165
Figure 4.23	Adsorption of Cu (II) on the OPF and OPFB at various pH_i	165

Figure 4.24	Removal of Cu (II) (50 mg/L) by the G and GB at various contact times	166
Figure 4.25	Removal of Cu (II) (50 mg/L) by the OPS and OPSB at various contact times	167
Figure 4.26	Removal of Cu (II) (50 mg/L) by the OPF and OPFB at various contact times	167
Figure 4.27	Removal of Cu (II) (10 mg/L) by the OPS and OPSB at various contact times	167
Figure 4.28	Removal of Cu (II) (30 mg/L) by the OPS and OPSB at various contact times	168
Figure 4.29	Removal of Cu (II) by the OPS and OPSB at various dosages	169
Figure 4.30	Removal of Cu (II) by the OPF and OPFB at various dosages	170
Figure 4.31	Liquid-solid mass transfer coefficient plots for the G and GB	179
Figure 4.32	Liquid-solid mass transfer coefficient plots for the OPS and OPSB	179
Figure 4.33	Liquid-solid mass transfer coefficient plots for the OPF and OPFB	180
Figure 4.34	External mass transfer diffusion model plots for the adsorption of Cu (II) by G and GB	181
Figure 4.35	External mass transfer diffusion model plots for the adsorption of Cu (II) by OPS and OPSB	182
Figure 4.36	External mass transfer diffusion model plots for the adsorption of Cu (II) by OPF and OPFB	182
Figure 4.37	Intraparticle diffusion of Cu (II) in G and GB	184
Figure 4.38	Intraparticle diffusion of Cu (II) in OPS and OPSB	184
Figure 4.39	Intraparticle diffusion of Cu (II) in OPF and OPFB	185
Figure 4.40	Pseudo-second order kinetic plots for the adsorption of Cu (II) by G and GB	187
Figure 4.41	Pseudo-second order kinetic plots for the adsorption of Cu (II) by OPS and OPSB	187
Figure 4.42	Pseudo-second order kinetic plots for the adsorption of Cu (II) by OPF and OPFB	188
Figure 4.43	Comparative plots of the measured and pseudo-second order modelled time profiles of the Cu (II) adsorption by OPS and OPSB	189

Figure 4.44	Comparative plots of the measured and pseudo-second order modelled time profiles of the Cu (II) adsorption by OPF and OPFB	189
Figure 4.45	Breakthrough curves of Cu (II) treated in the OPS- and OPSB-packed columns at various flow rates	191
Figure 4.46	Utilised capacity plots of the OPS- and OPSB-packed columns treating Cu (II) at various flow rates	192
Figure 4.47	Breakthrough curves of Cu (II) treated in the OPS- and OPSB-packed columns of various bed depths	193
Figure 4.48	Utilised capacity plots of the OPS- and OPSB-packed columns of various bed depths in the treatment of Cu (II)	193
Figure 4.49	Breakthrough curves of Cu (II) treated in the OPS- and OPSB-packed columns receiving various C_{in}	195
Figure 4.50	Utilised capacity plots of the OPS- and OPSB-packed columns treating Cu (II) of various C_{in}	196
Figure 4.51	Comparative utilised capacity of the OPS- and OPSB-packed columns during the adsorption-desorption and reutilisation experiment	197
Figure 4.52	Comparative elution process of the Cu (II) loaded OPS- and OPSB-packed columns utilising 0.1 M HNO_3	197

LIST OF PLATES

Plate 2.1	Sample of <i>Typha angustifolia</i> plantlet used in this research	30
Plate 2.2	The roots were touched gently against the wall of beaker to drip off excessive water for 15 sec	31
Plate 2.3	Excessive water were further removed by pressing the roots gently in between a folded paper towel for 1.5 min as shown	31
Plate 2.4	Weighing of the plantlet	32
Plate 2.5	Set up of the macro imaging system	34
Plate 2.6	The microcosm tanks with collapsible window at the 10 L marking above the tap	38
Plate 2.7	The various stages of below-ground plant biomass collection where media were separated	42
Plate 2.8	Separation of medium from dried below-ground plant biomass	42
Plate 2.9	The mesocosm system (the black tank is not a part of the system)	48
Plate 3.1	The G, GAC and Zeo samples	60
Plate 3.2	The OPS, CS and RH samples	60
Plate 3.3	The OPF, CF and SCF samples	61
Plate 3.4	The CCS, CFS and WS samples	61
Plate 3.5	The OPS sample (left) and its impurities	62
Plate 3.6	SEM image of G at 5000 ×	68
Plate 3.7	SEM image of Zeo at 5000 ×	68
Plate 3.8	SEM image of OPS at 1000 ×	69
Plate 3.9	SEM image of OPF at 1000 ×	69
Plate 3.10	SEM image of GAC at 1000 ×	70
Plate 3.11	SEM image of GAC at 20000 ×	70
Plate 3.12	The Day 29 effluents of the microcosms, mesocosm (labelled incubator) and pre-filtered sewage	81
Plate 3.13	The effluents of OPS-based microcosm (Days 5 – 90)	82

Plate 3.14	The effluents of OPF-based microcosm (Days 5 – 90)	82
Plate 3.15	Upwards growing roots in the OPF-based microcosm (Day 141)	83
Plate 3.16	The experimented media (GB, OPSB, OPFB, GACB and ZeoB)	84
Plate 3.17	SEM image of GB at 1000 ×	85
Plate 3.18	SEM image of OPSB at 1000 ×	85
Plate 3.19	SEM image of OPFB at 1000 ×	86
Plate 3.20	SEM image of GACB at 1000 ×	86
Plate 3.21	SEM image of ZeoB at 1000 ×	87
Plate 3.22	SEM image of a protozoon in ZeoB at 5000 ×	87
Plate 3.23	The plants in the middle columns were taller as seen on Day 97	91
Plate 3.24	Effect of distance from the inlets on the plants height as seen on Day 089	92
Plate 3.25	OPSB-A (top left), GB-A (top right), OPSB-B and GB-B	95
Plate 3.26	SEM image of OPSB-A at 500 ×	95
Plate 3.27	SEM image of OPSB-B at 500 ×	96
Plate 3.28	Area and spots of the SEM-EDX scanning at 200 ×	115
Plate 3.29	Surrounding area of Spot 2 (biggest lump in the middle) at 1000 ×	115
Plate 3.30	Area 2 of the SEM-EDX scanning at 200 ×	130
Plate 3.31	Surrounding area of Spot 1 (biggest lump in the middle) at 1000 ×	130
Plate 4.1	Media without (top) and with (bottom) biofilm formation	147
Plate 4.2	OPS, OPSB, OPSB-B and OPSB-A (anti-clockwise from upper-left)	147
Plate 4.3	SEM images of the G without (top) and with (bottom) biofilm formation at 200 x	148
Plate 4.4	SEM images of the OPS-based media without and with biofilm formation at 200 x	149
Plate 4.5	SEM images of the OPF without (top) and with (bottom) formation of biofilm at 200 x	150

Plate 4.6	SEM images of the GAC without (top) and with (bottom) formation of biofilm at 200 x	151
Plate 4.7	SEM images of the Zeo without (top) and with (bottom) formation of biofilm at 200 x	152

LIST OF SYMBOLS

\times	Magnification
\varnothing	Diameter
β_L	Liquid-solid mass transfer coefficient
Ω	Ohm
C	Concentration of sorbate
C_e	Concentration of sorbate at equilibrium
C_{ef}	Effluent concentration of sorbate
C_{in}	Influent concentration of sorbate
C_o	Initial concentration of sorbate
C_t	Concentration of sorbate at particular time
h	Initial adsorption rate
k_2	Pseudo-second order rate constant of adsorption
k_d	Intraparticle diffusion rate constant
K_F	Freundlich constant related to adsorption capacity
K_L	Langmuir constant related to adsorption affinity
k_L	Product of Q_m and K_L obtained from the Langmuir equation
m	Mass of sorbent per unit volume of sorbate
n	Freundlich constant related to adsorption intensity
pH_e	pH at equilibrium
pH_i	Initial pH
Q_e	Adsorption capacity at equilibrium
$Q_{e\text{ cal}}$	Q_e calculated from the regressed equation
$Q_{e\text{ exp}}$	Q_e obtained from the experiment
Q_m	Maximum adsorption capacity
Q_t	Adsorption capacity at particular time
R^2	Regression coefficient

R_L	Separation factor obtained from Langmuir isotherm model
S	Surface area for mass transfer / specific particle surface
t	Time
t_e	Time when adsorption equilibrium is achieved
v/v	Volume per volume ratio
W	Watt
w/w	Weight per weight ratio
x_e	Average removal efficiency at equilibrium

LIST OF ABBREVIATIONS

BET	Brunauer-Emmet-Teller
B _G	Physico-chemistry property difference of GB - G
B _{GAC}	Physico-chemistry property difference of GACB - GAC
B _{OPF}	Physico-chemistry property difference of OPFB - OPF
B _{OPS}	Physico-chemistry property difference of OPSB - OPS
B _{Zeo}	Physico-chemistry property difference of ZeoB - Zeo
CCS	Coarse sand (processed medium)
CF	Coconut mesocarp fibre (processed medium)
CFS	Fine sand (processed medium)
CS	Coconut shell (processed medium)
CSLM	Confocal scanning laser microscopy
CSPI	Center for Science in the Public Interest
EDX	Energy dispersive x-ray
EFB	Empty fruit bunch
EPA	Environment Protection Agency
EPS	Extracellular polymeric substances
EQA	Environmental Quality Act
FAAS	Flame atomic absorption spectrometer
FOS	Focus on Surfactants
FT-IR	Fourier transformed infra-red
G	Gravel (processed medium)
GAC	Granular activated carbon (processed medium)
GACB	Biofilmed GAC
GB	Biofilmed G
GEC	General Electric Company
HLR	Hydraulic loading rate

INT	Iodonitrotetrazolium
LRB	Legal Research Board
M	Mean of the measurements
MCLG	Maximum contaminant level goals
MPOB	Malaysian Palm Oil Board
O.C.T.	Optimal cutting temperature
OPF	Oil palm mesocarp fibre (processed medium)
OPFB	Biofilmed OPF
OPS	Oil palm shell (processed medium)
OPSB	Biofilmed OPS
PLASMA	Malaysian Oil Palm Training Centre
POIC	Palm Oil Industrial Cluster
POME	Palm oil mill effluent
PP	Polypropylene
PVC	Polyvinyl chloride
RH	Rice hull (processed medium)
RM	Ringgit Malaysia
rpm	Revolution per minute
RSD	Relative standard deviation
SCF	Sugarcane fibre (processed medium)
SD	Standard deviation
SEM	Scanning electron microscope
SF	Surface flow
SSF	Subsurface flow
SUSSC	Special Unit for South-South Cooperation
TGA	Thermogravimetry analyser
UMS	Universiti Malaysia Sabah
UNCED	United Nations Conference on Environment and Development

USD	US Dollar
USM	Universiti Sains Malaysia
WCED	World Commission on Environment and Development
WS	Wood shave (processed medium)
Zeo	Zeolite (processed medium)
ZeoB	Biofilmed Zeo

LIST OF APPENDIXES

Appendix 1	Experimental Results	222
Appendix 2	Photographical Evidence of the <i>Typha angustifolia</i> Growth in Various Experimental Constructed Wetland Units	266
Appendix 3	Langmuir and Freundlich Adsorption Isotherm Models	267
Appendix 4	Photographical Evidence of the Biofilm Formation	268
Appendix 5	Secondary Data for Chapter 4	282

**PENCIRIAN ASAS TEMPURUNG KELAPA SAWIT SEBAGAI MEDIUM PAYA
BINAAN DAN KESAN PEMBENTUKAN BIOFILM TERHADAP
PENJERAPAN KUPRUM (II) PADA MEDIUM**

ABSTRAK

Kajian ini dilakukan untuk menilai potensi tempurung kelapa sawit sebagai medium paya binaan dan menyelidik kesan pembentukan biofilm pada medium ini terhadap penjerapan kuprum (II). Mikrokosm berasaskan tempurung kelapa sawit ditanam dengan anak *Typha angustifolia* dan dibiarkan terdedah pada iklim tropika bersama-sama dengan mikrokosm-mikrokosm berasaskan medium lain. Kesemua mikrokosm ini dipantau selama satu setengah tahun. Didapati mikrokosm berasaskan tempurung kelapa sawit adalah superior dari segi tumbesaran ketinggian, penjanaan pucuk dan pertambahan berat kering pokok. Tempurung-tempurung kelapa sawit tanpa biofilm dan berbiofilm kemudiannya dikaji menerusi siri ujikaji kelompok dan turus. Data ujikaji mematuhi model Langmuir; kapasiti penjerapan maksimum tempurung kelapa sawit tanpa biofilm dan berbiofilm masing-masing adalah 5.29 mg/g dan 4.88 mg/g. Kedua-dua medium ini memberikan pekali regresi melebihi 0.98 apabila data ujikaji masing-masing diaplikasikan ke dalam persamaan tertib pseudo-kedua, mencadangkan lebih daripada satu parameter kawalan terlibat dalam proses penjerapan. Keupayaan penjerapan medium ini boleh dijana semula menerusi proses pengelusan mudah dengan menggunakan 0.1 M HNO₃ sebagai pengelusi, menunjukkan kebolehpanjangan jangka hayat medium penjerap ini dan potensi perolehan semula logam yang terjerap. Walau bagaimanapun, biofilm yang terbentuk pada tempurung kelapa sawit secara amnya telah merendahkan prestasi penjerapan dan dapatan ini diterangkan dengan mencadangkan disebabkan oleh kesan halangan. Berdasarkan parameter-parameter yang dikaji, tempurung kelapa sawit didapati sesuai untuk kegunaan paya binaan. Namun demikian, kesan sampingan sementara yang dibincangkan perlu diambilkira sebelum menggunakan medium ini dalam sistem paya binaan untuk rawatan air sisa berskala penuh.

**BASIC CHARACTERISATION OF OIL PALM SHELL AS CONSTRUCTED
WETLAND MEDIA AND THE EFFECT OF BIOFILM FORMATION
ON ITS ADSORPTION OF COPPER (II)**

ABSTRACT

This study was conducted to assess the potential of oil palm shell as constructed wetland media and to investigate the effect of biofilm formation on the oil palm shell on its adsorption of copper (II). The oil palm shell-based microcosm was planted with *Typha angustifolia* plantlets and left outdoor in tropical environment together with other media-based microcosms. These microcosms were monitored for a period of one and a half years. The oil palm shell-based microcosm was found to be superior in terms of plant height growth, shoot generation rate and dry biomass gain. The non-biofilmed and biofilmed oil palm shell were then experimented via a series of batch and column experiments. The experimental results obeyed the Langmuir model; the non-biofilmed and biofilmed oil palm shell were found to have the maximum adsorption capacity of 5.29 mg/g and 4.88 mg/g, respectively. Both these media gave the regression coefficients over 0.98 when their experimental results were applied to the pseudo-second order equation, suggesting that more than one rate controlling step were involved in their adsorption processes. Their adsorption capabilities can be regenerated upon exhaustion via a simple elution process utilising 0.1 M HNO₃ as the eluent, indicating the extendable lifespan of these sorbents as well as the potential recovery of the metal adsorbed. However, the biofilm formed on the oil palm shell has generally caused its adsorption performance to reduce and this was explained by proposing the barrier effect. Based on the parameters studied, the oil palm shell is concluded to be suitable for constructed wetland application; nonetheless, the temporary impacts discussed must be taken into consideration before utilising it in a full scale constructed wetland system for wastewater treatment.

CHAPTER 1

INTRODUCTION

This research is intended to support the theme sustainable development and green technology (UNCED, 1992; WCED, 1987). It is hoped to deliver some contribution to academia in these fields as well. The local situation in Sabah, where the researcher did his early tertiary educations and currently working in, has aroused and propelled the initial ideas. Further ideas were developed and experimented in Universiti Sains Malaysia (USM), Penang.

1.1 The Birth of Idea

The series of field trips dated back to 1998 (when the researcher was in his second undergrad year) has given birth to the initial ideas in this work where the series of environmental issues and observations were merged together to form a possible win-win solution.

There was this Lohan tailing's dam which is famous among the local residents of Lohan-Ranau area where there were rumours about environmental heavy metal pollution inflicted by copper mining activity. Since the tailings were transported via pipeline from Mamut copper mine to Lohan tailing's dam; water were used to ease the flow and this resulted in diluted effluent which comply to the Environmental Quality Act (EQA) 1974 (LRB, 2004) requirement. The effluent was discharged directly via the overflow of the tailing's retention dam into Lohan River without any treatment then.

The Lohan River is a high flowing river throughout the year, thus the environmental pollution was masked. Fortunately today, the mine has ceased its operation. The Mamut open pit mine is now a lake and the Lohan tailing's dam is now a dumpsite planted with *Typha* spp. mimicking a freshwater wetland. Although this local issue is not a tragedy like what has happened at Minamata Bay but it is still a long term micro-dose exposure of heavy metal to the local environment, especially the residual copper, which could have been prevented (Chen *et al.*, 1996).

In 1999, new copper prospects were discovered next to Mamut. There is no mining until today; however, there is no warranty that it would not happen in future when the copper price is attractive enough to lure miner. If mining took place one day, it would be good to retain the micro-dose of heavy metal before discharging the effluent into any river. The most economical way is to use cheap biosorbent and/or heavy metal precipitation inducing medium and let the environment fix itself naturally.

In search of biosorbent, the cheapest would be the unwanted material. Coincidentally, there is a lot of oil palm waste available in Malaysia. Empty fruit bunch (EFB), palm shell and mesocarp fibre are normally utilised as fuel to generate electricity via mill's boiler. Although the oil palm mesocarp fibre yields less heat than the shell, it is normally the first to be burnt as it will be a nuisance if wind blows it around. As a result, excessive oil palm shell remained, some are used for road surfacing in the mill and its surrounding while some often caught fire. By common sense, the oil palm shell contains fatty products and should adsorb heavy metal. If anyone were to remove low dose of heavy metal by utilising oil palm shell, the operation must be economical otherwise it would not be feasible.

Any economical operation must be energy and man power saving, and low maintenance (self organising). A design that mimics a column or filter bed to contain the biosorbent and the heavy metal laden water in it simultaneously is needed in order to enable adsorption process to take place. Coincidentally again, there is a sizeable lake behind the School of Science and Technology, Universiti Malaysia Sabah (UMS). Although this lake was created to trap silts during heavy down pour, it functions as freshwater wetland most of the time purifying water in it and provides habitats for small wildlife as the wetlands in Putrajaya. And thus, the idea of experimenting oil palm shell as constructed wetland media to adsorb the copper was born.

1.2 Constructed Wetland

1.2.1 Definition

A constructed wetland is a designed and man-made complex of saturated substrate, emergent and/or submergent vegetation, animal life and water that simulate natural wetlands for human use and benefits (Ho, 2002). There are many other versions of definition available today; however, it is generally agreed that constructed wetland is an artificial engineered piece of “land” which is saturated with water, developed to mimic the natural wetland for various purpose of mankind such as water treatment and landscaping.

Among the scientific community, constructed wetland could be vegetated or unvegetated (Artsanti, 2005; Huett *et al.*, 2005; Karathanasis *et al.*, 2003; Tong and Sikora, 1995) and terms such as microcosm (Yang *et al.*, 2001; Gillespie *et al.*, 1999; Ingersoll and Baker, 1998), mesocosm (Ahn *et al.*, 2001; McBride and Tanner, 2000) and macrocosm (Bachand and Horne, 2000) refer to the small scale experimental units

of the constructed wetland system (normally vegetated) which simply mean micro, meso and macro ecosystem, respectively.

1.2.2 Basic components

At the very minimum, constructed wetland must consist of at least substrate and water. The substrate refers to the medium that provides physical support for the plants and microbial attachments. Throughout this thesis, the word “media” and “sorberent” are used interchangeably with “substrate”. The second component is water which contributes its “wetness”. Because constructed wetland is a non-sterile environment which exposed to air. Microbial growths in the media-water phase which form the biofilm is unavoidable; thus, the third component (Artsanti, 2005). The unvegetated constructed wetland is also known as filter bed.

Typically, constructed wetland is vegetated with aquatic plant. In constructed wetland research, it is normally agreed that the basic components of a constructed wetland are the media, waterbody and plant, which in turn became the adjustable parameters for the research such as the type of media used (Drizo *et al.*, 2006; Prochaska and Zouboulis, 2006; García *et al.*, 2003; Scholz and Xu, 2002a; Brooks *et al.*, 2000; Gray *et al.*, 2000), type of wastewater fed (Dunne *et al.*, 2005; Ahmad *et al.*, 2003; Mays and Edwards, 2001) and other hydraulic properties (Tao *et al.*, 2006; Jenkins and Greenway, 2005; García *et al.*, 2003), and type of plant used (Gottschall *et al.*, 2007; Akrotos *et al.*, 2007; Iamchaturapatr *et al.*, 2007; Bragato *et al.*, 2006; Karathanasis *et al.*, 2003). There are various experimental mathematical simulation models that derived from these adjustable parameters available for specific purposes today (Stein *et al.*, 2006; Mayo and Bigambo, 2005; Marsili-Libelli and Checchi, 2005;

Wynn and Liehr, 2001; McBride and Tanner, 2000; Kadlec, 2000; Werner and Kadlec, 2000; Mitsch and Wise, 1998).

1.2.3 Design

Constructed wetland designs include horizontal surface and sub-surface flow, vertical flow, floating raft and batch system (Ragusa *et al.*, 2004; Shutes *et al.*, 2002). Surface flow (SF) wetland is similar to the natural marsh and is normally planted with macrophytes. In sub-surface flow (SSF) wetland, wastewater flows horizontally or vertically through the substrates. The SSF system is more effective than the SF system at removing pollutants at high application rates (Shutes *et al.*, 2002); which also explain why most wastewater treatment research experimental designs are of SSF system. Nonetheless, the batch system is gaining popularity in small scale research as it is relatively easier and cheaper to operate (Stein *et al.*, 2006; Grove and Stein, 2005; Ragusa *et al.*, 2004; Nelson *et al.*, 1999). Various flow-designs of constructed wetland system may be combined (hybrid system) in order to achieve higher treatment effect, especially for nitrogen removal (Vymazal, 2005; Pastor *et al.*, 2003).

The technical aspects of system design and treatment efficiency rely mostly on the hydraulic behaviour. The easiest way to optimise a constructed wetland wastewater treatment system is to maximise the hydraulic flow path by manipulating its inlet-outlet position (Suliman *et al.*, 2006; Somes and Wong, 1997). Another typical method is to optimise the contact time and/or contact surface area between the media (including biofilm), plant rooting matrix and wastewater. This type of optimisation is normally done by adjusting the aspect ratio of the constructed wetland system, hydraulic loading rate (HLR), media size, and water or media depth (Maloszewski *et al.*, 2006; García *et al.*, 2005; García *et al.*, 2004; Pastor *et al.*, 2003). To further exploit

the hydraulic flow path, one can actually adopt different strategies of filling the media into the constructed wetland (Suliman *et al.*, 2007).

The bed depth of the constructed wetland system varies depending on the design and purpose of the intended treatment or study which could be 15 cm (Manyin *et al.*, 1997), 20 cm (Wild *et al.*, 2001), 27 cm (García *et al.*, 2005), 30 cm (Ingersoll and Baker, 1998), 35 – 40 cm (Groudeva *et al.*, 2001), 40 cm (Ahn *et al.*, 2001), 45 cm (Akratos and Tsihrintzis, 2007; Yang *et al.*, 2001), 50 cm (Price and Probert, 1997; Tong and Sikora, 1995), 60 cm (Peverly *et al.*, 1995) *etc.* Nonetheless, Shutes *et al.* (1997) recommended the minimum bed depth of 60 cm for full scale SSF system.

1.2.4 General applications

Constructed wetland was initially developed to exploit and improve the biodegradation ability of plants. Constructed wetland wastewater treatment technology may be relatively slow compared to conventional wastewater treatment technology; however, it offers low construction and operating cost, and is appropriate both for small communities and as a final stage treatment in large municipal systems (Shutes *et al.*, 2002; Kivaisi, 2001). The role of constructed wetland in sustainable development (Price and Probert, 1997) as well as its challenges (Bavor *et al.*, 1995), advantages and disadvantages (Gopal, 1999; Verhoeven and Meuleman, 1999; Brix, 1999) have been discussed by numerous authors.

The performance of constructed wetland system is normally influenced by its area, length to width ratio, water depth, HLR and hydraulic retention time (HRT). Efficiency above 90% is normally achieved for the removal of pathogenic microorganisms, an expectable 80% for the removal of organic materials and

suspended solids; however, nutrient removal efficiency is normally below 60% (Shutes, 2001). Heavy metal removal is often above 70% (Lim *et al.*, 2003b).

Over the years, constructed wetland technology has been utilised in many parts of the world. As tabulated in Table 1.1, researches on constructed wetland wastewater treatment systems are gaining interest in many areas of water pollution control. Due to its versatility, it is common to treat more than a pollutant simultaneously; this is especially true with the advancement of the hybrid design (Vymazal, 2005).

Table 1.1: Examples of various pollutants treated utilising constructed wetland wastewater treatment system

Pollutants	Selected references
Oxygen demand	Caselles-Osorio and García, 2006; Karathanasis <i>et al.</i> , 2003; Lim <i>et al.</i> , 2003a; Ji <i>et al.</i> , 2002; Lim <i>et al.</i> , 2001
Solids	Ansola <i>et al.</i> , 2003; Braskerud, 2003; Karathanasis <i>et al.</i> , 2003
Nutrient	Gottschall <i>et al.</i> , 2007; Akratos and Tsihrantzis, 2007; Vymazal, 2007; Kootatep and Polprasert, 1997
Heavy metal	Maine <i>et al.</i> , 2006; Ahmad <i>et al.</i> , 2003; Lim <i>et al.</i> , 2003b; Scholz and Xu, 2002b; Lim <i>et al.</i> , 2001; Groudeva <i>et al.</i> , 2001
Organic	Davies <i>et al.</i> , 2006; Grove and Stein, 2005; Runes <i>et al.</i> , 2003; Groudeva <i>et al.</i> , 2001; Pinney <i>et al.</i> , 2000
Pathogen	Wand <i>et al.</i> , 2007; Keffala and Ghrabi, 2005; Karim <i>et al.</i> , 2004; Mayo, 2004; García <i>et al.</i> , 2003; Cheng <i>et al.</i> , 2002a
Landfill leachate	Ahmad <i>et al.</i> , 2006a; Ahmad <i>et al.</i> , 2006b; Bulc, 2006; Ahmad <i>et al.</i> , 2003
Urban run off	Shutes <i>et al.</i> , 1997
Explosives	Best <i>et al.</i> , 1999

1.2.5 Treatment of heavy metal

Heavy metal toxicity is a function of both concentration and form (Murray-Gulde *et al.*, 2005). Natural wetland is an effective sink for heavy metal and so do constructed wetland (Dunbabin and Bowmer, 1992). There are results of 16 years monitoring that show that constructed wetland is efficient and stable in purifying heavy metal contaminated wastewater (Yang *et al.*, 2006). Other evidences on heavy metal

removal (in special reference to lead, Pb) utilising wetland technology is available in the literature by Odum (2000).

Unlike the removal of heavy metal in conventional wastewater treatment system, the mechanism of heavy metal removal in wetland system is much more complicated and it involves at least six mechanisms that happen simultaneously as described in the paragraphs hereafter. Conceptual models for predicting heavy metal removal performance in a constructed wetland system have been presented by at least two teams of researchers (Lee and Scholz, 2006; Flanagan *et al.*, 1994).

The moment heavy metal laden wastewater enters a constructed wetland system; it is subjected to physical filtration. The plant and media slow the flow of water through the system, allowing fine particles to settle out. Emergent plants as well as the substrate may trap and retain sediments, and prevent turbulent resuspension. Therefore, it is common to find that heavy metal concentration in wetland substrate decrease along the course of treatment with its highest concentration at the inlet's surrounding (Cheng *et al.*, 2002b; Obarska-Pempkowiak and Klimkowska, 1999).

Because the wetland substrate is most likely to contain humic substance, complexation of heavy metal ion-humic substance will occur. At the same time, due to the presence of microbes; microbial mediation reactions will take place with the heavy metal ion via oxidation, reduction and biosorption. These two mechanisms eventually lead to the precipitation of insoluble heavy metal sulphides where oxygen is low at the bottom of the substrata (Hallberg and Johnson, 2005a and 2005b; Walker and Hurl, 2002; Groudeva *et al.*, 2001; Groudev *et al.*, 1999; Sobolewski, 1996).

The simplest way of treating heavy metal laden water is via adsorption; it is sometimes known as biosorption when a biological entity or mass is the sorbent. In

wetland system, heavy metal ion is attracted to the negative charge of the organic material as well as the biofilm (Wood and Shelley, 1999; Machemer and Wildeman, 1992). However, adsorption plays a small overall role in the removal of heavy metal in wetland system unless at the initial stage where the organic and microbial abundance is low. Therefore, it is not necessary to employ expensive high sorptive media as a constructed wetland media (Scholz, 2003).

The last, but not less important, mechanism of removal is plant uptake. Over the years, researchers have proven the ability of macrophytes in uptaking heavy metal from wastewater. However, the heavy metal uptake by plant contributes only a small part of heavy metal removal in constructed wetland system with the highest uptake occurs in the root zone where the plant is in direct contact with the heavy metal laden wastewater (Bragato *et al.*, 2006; Fritioff and Greger, 2006; Mays and Edwards, 2001; Scholes *et al.*, 1998; Mungur *et al.*, 1995). Manios *et al.* (2003) found that the heavy metal accumulated in the plant does not exhibit any toxic effect to the plant itself. When the plant dies, it provides organic material to the system, thus providing carbon source to the microbial community as well as organic adsorption site for further heavy metal adsorption (Batty and Younger, 2007).

1.3 Malaysia Oil Palm Scenario

Indigenous to Africa, the oil palm (*Elaeis guineensis*) has been domesticated from the wilderness and transformed to become a plantation-based industry (SUSSC, 2001). Its commercial value lies mainly in the oil that can be obtained from the mesocarp of the fruit (palm oil) and the kernel of the nut (palm kernel oil). Palm oil is used mainly for cooking (cooking oil, margarine *etc.*) and has non-food (soap, detergent, cosmetics *etc.*) applications.

The first commercial oil palm estate in Malaysia was set up in 1917 at Tennamaran Estate, Selangor (SUSSC, 2001). The growth of the industry has been phenomenal and Malaysia is now the largest producer and exporter of palm oil in the world, accounting more than half of the world's production with the total cultivated land area of approximately 3,800,000 ha (UMS, 2006).

Exactly a decade ago, the Malaysian palm oil production was around 9,000,000 ton (FOS, 2006); this figure has escalated to an average of 15,600,000 ton throughout the 2001 – 2005 seasons, and the production volume was 15,700,000 ton in 2006 (Zaidi and Ooi, 2006). Figure 1.1 illustrates these production figures over the period of 2001 – 2006. The Malaysian government is expanding production in eastern Malaysia, in special reference to the state of Sabah, as the growing importance of the crop is boosted by the need for palm oil-derived biodiesel (FOS, 2006).

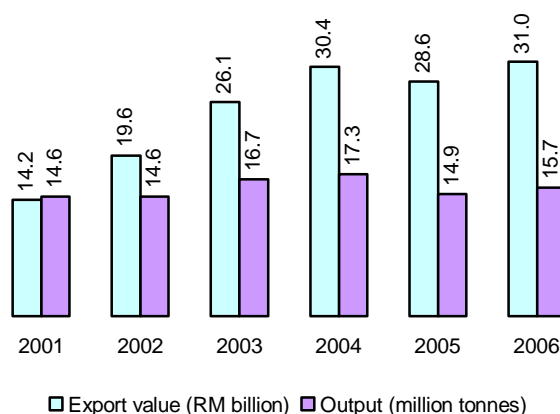


Figure 1.1: Malaysia's palm oil highlights (Zaidi and Ooi, 2006)

The expansion of oil palm estate has caused changes in landuse (McMorrow and Mustapa, 2001). It sometimes may have directly or indirectly caused human-wildlife conflict where original forest land is cleared for oil palm planting. In such case, habitat is destroyed, migration patterns may be hindered and travel corridors may be

blocked (CSPI, 2005). This implication is less if the land were previously already a rubber or cocoa plantation.

The main by-products and wastes produced from the processing of oil palm are EFB, palm oil mill effluent (POME), sterilizer condensate, mesocarp fibre and shell. Both EFB and POME have been used extensively as organic fertiliser in oil palm estate while the mesocarp fibre and shell are used as fuel, making the mill self-sufficient in energy (Mahlia *et al.*, 2001). The shell has also been used for road surfacing in estate.

1.3.1 Sabah oil palm sector

The state of Sabah, situated in North Borneo, is the biggest planter of oil palm in Malaysia with a planted land area of 1,209,368 ha as in 2005 (Hisamuddin, 2006) and it is setting itself to become the leading palm oil-based biodiesel player in the world when the Palm Oil Industrial Cluster (POIC) goes into full swing (Chris, 2006). Lahad Datu has been identified as the palm oil industry hub of Sabah and Sarawak, and the Malaysian Oil Palm Training Centre (PLASMA – Pusat Latihan Sawit Malaysia) is established here as the government's effort to assist in the development of the oil palm industry in Sabah and Sarawak via human capital development (MPOB, 2006).

1.4 Copper

Copper (Cu) is an essential nutrient to all higher plants and animals. In humans, it is found primarily in the bloodstream as a cofactor in various enzymes and in Cu-based pigments. However, the United States Environmental Protection Agency (EPA, 2006) has found Cu to potentially cause the following health effects when people are exposed to it at levels above the Maximum Contaminant Level Goals (MCLG).

Short periods of exposure can cause gastrointestinal disturbance, including nausea and vomiting. Use of water that exceeds the MCLG over many years could cause liver or kidney damage. The MCLG for Cu has been set at 1.3 mg/L. In Malaysia, the Environmental Quality Act (EQA) 1974 (Act 127) has set the levels of 0.2 mg/L and 1.0 mg/L for Standard A and Standard B effluents, respectively (LRB, 2004).

This particular metal, Cu, has found a wide range of applications and is in high market demand. Its price has quintupled since 1999, rising from USD 0.60/lb in June 1999 to USD 3.75/lb in May 2006 where it began to drop steadily, most recently dropping below USD 3.00/lb in December 2006 (MetalSpotPrice.com, 2007).

1.4.1 Mamut copper mine

Mamut copper mine, the largest open pit mine in Malaysian history is located at northwest of Sabah about 68 km east of Kota Kinabalu, which is an equivalent of approximately 120 km by road. The open pit and its facilities are located at the southeast of Mount Kinabalu, at the elevation of 1300 – 1600 m above sea level (Mohd. Azizli *et al.*, 1995).

Mamut was a medium size porphyry copper-gold (Cu-Au) deposit with the pre-mining reserve of 130,000,000 ton at a grade of 0.52% Cu and 0.56 g/ton of gold (Au). Other porphyry copper mining operations in South East Asia include Grasberg in Irian Jaya, Batu Hijau in Indonesia and Padcal in the Philippines (Perilya, 2006).

The Mamut was mined at a rate of 6,000,000 ton annually in a 24 years operation that ended in October 1999 to produce 580,000 ton of Cu, 300 ton of silver

(Ag) and 1,400,000 oz of Au (Perilya, 2006). Throughout the operation it has earned more than RM 3 billion in export revenue for Malaysia (Tan, 2006).

Nonetheless, a common environmental issue associated with the mineral industries is the disposal and management of enormous masses of tailings from their processing operations. In this case, the Lohan tailing's dam has a total site area of about 400 ha and is located 15 km east of the mine (Mohd. Azizli *et al.*, 1995). Indigenous residents in 17 villages throughout the Lohan area charged that the mine has hurt the fertility of their land, polluted their rivers and water supplies, and endangered their health (Weissman, 1994).

Mining activities ceased in October 1999 and environmental protection measures has been carried out to safeguard the interest of the surrounding residents. The state government claimed that there is no problem with the quality of water for consumption and it has invited investor to develop the abandoned 4800 ac mine site into a resort development project. Local university campus was also proposed to be erected at the Lohan tailing's dam site (Sabah government, 2001).

On the other hand, there are new copper prospects discovered in early 1999 at Bongkud, Junction and Naping (which collectively known as Tampang Project) close to the township of Ranau. These prospects consist of coincident Cu-Au in soil and geophysical anomalies that occurs to be associated with intrusive stocks along the 5 km west-northwest trending Tampang trend structural corridor which situated in an area of granodiorite intrusion, collectively referred to as the Kinabalu Magmatic Zone (Perilya, 2006).

1.5 Biofilm

1.5.1 Definition

Most microorganisms live and grow in aggregates such as biofilm, floc (“planktonic biofilms”) and sludge. This form of microbial life is described by the somewhat inexact but generally accepted term “biofilm” (Flemming *et al.*, 2000). Earlier researchers have used other terms such as microbial or biological film, wall growth and microbial slimes instead of biofilm (Bryers, 2000a). Throughout this thesis, the term biofilm is defined according to Characklis and Marshall (1990) as a surface accumulation, which is not necessarily uniform in time or space that comprises cells immobilised at a substratum and frequently embedded in an organic polymer matrix of microbial origin.

1.5.2 Formation

Although biofilm can occur in the form of floating mats on liquid surfaces, it is normally found on solid substrates submerged in or exposed to some aqueous solution. In a favourable condition, biofilm will quickly grow to be macroscopic. But before that, how does biofilm formed?

Initially, the substratum is conditioned and microbial cells attach reversibly, then irreversibly. The attached cells grow, reproduce and secrete insoluble extracellular polysaccharidic material to form a layer of biofilm. As the biofilm matures, biofilm detachment and growth process come into balance, such that the total amount of biomass on the surface remains approximately constant in time (Bryers, 2000b). Details on structural determinants in biofilm formation are available in the written work of Wimpenny (2000).

Figure 1.2 graphically represents the processes governing biofilm formation and persistence which include the following steps.

1. Biasing or preconditioning of the substratum either by macromolecules present in the bulk liquid or intentionally coated on to the substratum.
2. Transport of planktonic cells from the bulk liquid to the substratum.
3. Adsorption of cells at the substratum for a finite time followed by,
4. Desorption (release) of reversibly adsorbed cells.
5. Irreversible adsorption of bacterial cells at a surface.
6. Transport of substrates to and within the biofilm.
7. Substrate metabolism by the biofilm-bound cells and transport of products out of the biofilm. These processes are accompanied by cellular growth, replication, and extracellular polymer production.
8. Biofilm removal (detachment or sloughing).

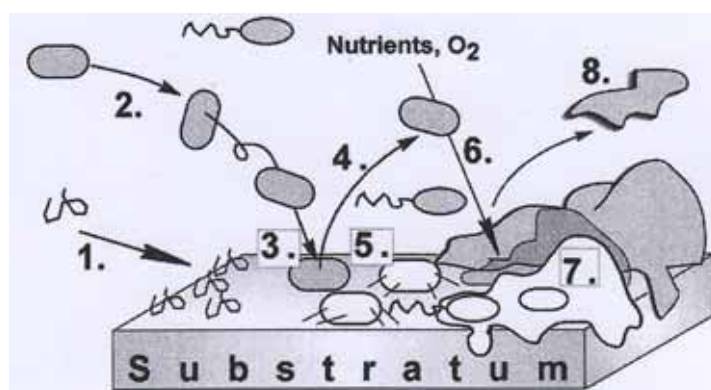


Figure 1.2: Processes governing biofilm formation (Bryers, 2000b)

According to Tao *et al.* (2006), it took 1 – 6 weeks or less for maturation of the biofilm on submerged plant surfaces and the sedimentary microbial community in a constructed wetland system.

1.5.3 Conceptual models

According to Lewandowski (2000), traditional conceptual of biofilm was that microorganisms are uniformly distributed in a continuous matrix of extracellular polymer. Unfortunately, this model could not interpret the collections of microscale experimental results. As a result, new conceptual model of heterogeneous biofilm has been suggested, that biofilm consists of microcolonies separated by interstitial voids (Figure 1.3).

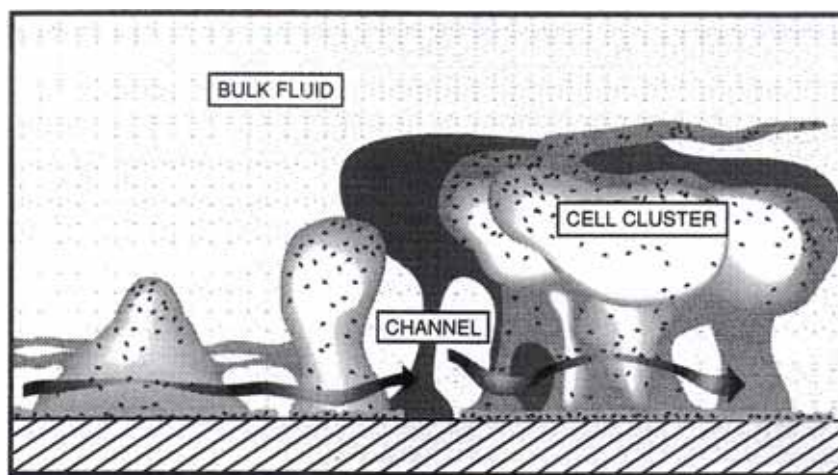


Figure 1.3: Diagrammatic representation of the structure of the hypothetical bacterial biofilm drawn from confocal scanning laser microscopy (CSLM) examination of a large number of mono- and mixed-species biofilms. The discrete microcolonies of microorganisms are surrounded by a network of interstitial voids filled with water. The arrows indicate convective flow within the water channels (Lewandowski *et al.*, 1995)

1.5.4 Extracellular polymeric substances

Apart from biochemical and biological, biofilm also display physical and physico-chemical properties which are chiefly caused by the extracellular polymeric substances (EPS, also known as exopolysaccharide) that fill the space between the cells and account for a considerable proportion of the biofilm's organic carbon content. The EPS consist of polysaccharides and considerable amounts of protein, nucleic acids and

lipids. Importantly, the EPS provide a matrix which allows the cells to maintain their position for a much longer period of time compared to planktonic mode; thus it forms the morphology and internal structure of biofilm. The binding forces that contribute to the mechanical stability in biofilm are summarised in Figure 1.4. A detailed documentation on EPS is available in the writing of Flemming *et al.*, (2000).

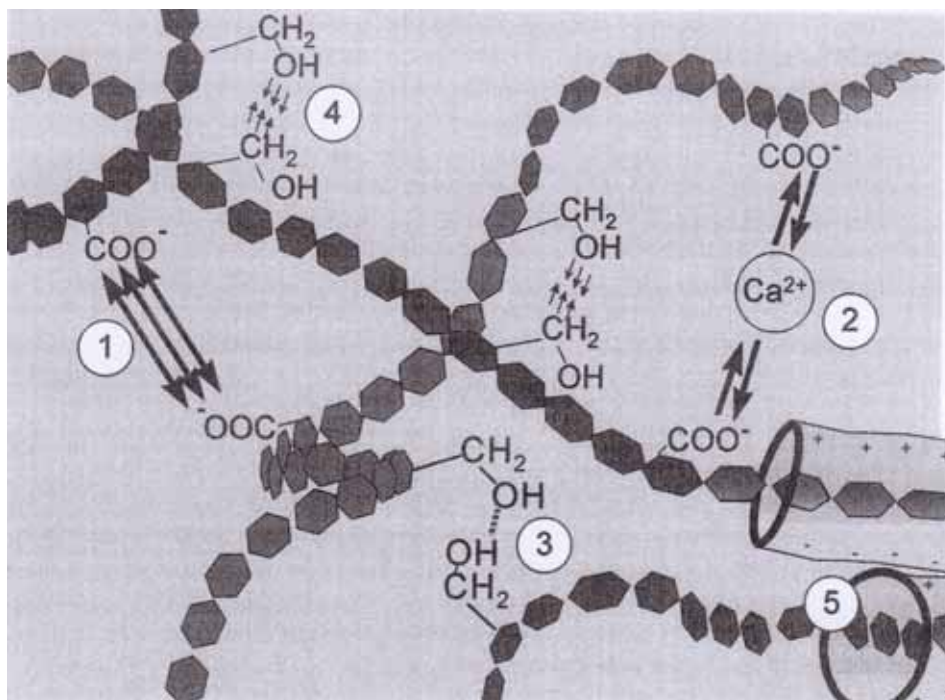


Figure 1.4: Proposed model for dominating intermolecular interactions which contribute to mechanical stability in a biofilm. Five different phenomena are considered. 1 = repulsive electrostatic interactions between ionic residues; 2 = attractive electrostatic forces, typically in the presence of divalent cations; 3 = hydrogen bonds; 4 = other electrostatic interactions, e.g. between dipoles; 5 = London (dispersion) interactions (Flemming *et al.*, 2000)

1.5.5 Persistency

Biofilm is ubiquitous. Nearly every species of microorganism has mechanisms by which they can adhere to surfaces and to each other. Biofilm exist almost everywhere, as long as there is the presence of moisture or water, and it is highly

hydrated with a ratio of 1 – 2% to 98% (w/w) water is common (Christensen and Characklis, 1990).

In our daily life, biofilm exist in our mouth as dental biofilm which causes dental decay. The slimy substance (which typically invisible to naked eyes) on our fish tank wall as well as the rocks in the pool are all biofilm of their own kind. Biofilm can also exist in hot spring (Chong, 2001). In the industrial sector, biofilm is normally a set back as it decreases process efficiency and is costly to manage. In the medical field, biofilm is often associated with disease and persister cell where it has caused some problems that antibiotic does not seems to work. However, biofilm is useful in the process of water treatment to treat organic related pollutants.

1.5.6 Notes on biofilm-heavy metal

Biofilm is able to accumulates and binds heavy metal ions from the passing water due to the physico-chemical properties of its microbial molecules and microbial metabolism, which involve processes such as transport across the cell membrane, biosorption to cell walls and entrapment in extracellular capsules, metabolically-induced precipitation, complexation and oxidation-reduction reactions (Alvarez *et al.*, 2006; Hallberg and Johnson, 2005b; Bremer and Geesey, 1993; Hughes and Poole, 1989). Anionic group such as carboxyl, phosphoryl and sulphate groups which offer cation exchange potential may presence in EPS. This explains why a wide variety of metal ions are reportedly bound to EPS. It is interesting to note that theoretical predictions of metal binding capacities are based on the estimated numbers of available carboxyl and hydroxyl groups (Flemming *et al.*, 2000). Metal uptake appeared to be predominantly a feature of the level of EPS production and attachment rather than metabolic sponsored activity (Scott *et al.*, 1995).

According to Dugan (1975 cited in Flemming *et al.*, 2000), EPS have shown to accumulate up to 25% their weight as metal ions. Adsorption densities as high as 22 ng/mg have been reported for Cu (Kaplan *et al.*, 1987) and an amazing bioconcentration factors between 10^2 to 6×10^4 for various heavy metals have been recorded for riverine biofilm (Frieze *et al.*, 1997). Costley and Wallis (2001) discovered that the heavy metal accumulation in biofilm is extracellular and its adsorption capacity did not appear to be adversely affected by adsorption-desorption processes making it a tool to remove and recover heavy metal from wastewater.

In studies of freshwater lakes, biofilm under near-neutral pH scavenged metals up to 12 orders of magnitude higher than biofilm under lower pH conditions (Ferris *et al.*, 1989). Fuchs *et al.*, (1997) have recommended a method utilising biofilm as a practical instrument for assessing heavy metal pollution in fresh water ecosystems. The recent advancement in biofilm research came in the work of Ragusa *et al.*, (2004) where they managed to assess the biofilm growth by utilising its total protein, EPS, viable cells and *p*-Iodonitrotetrazolium Violet (INT) reduction rates as indicators.

1.6 Research Objectives

It is generally agreed that primary mechanisms of heavy metal removal in constructed wetland are via chemical precipitation (by formation of or co-precipitation with insoluble compounds) and adsorption (onto substrate and plant surfaces) while the secondary mechanism is via plant uptake (Stowell *et al.*, 1981 cited in Lim and Polprasert, 1998). Lim and Polprasert (1998) summarised that:

- the removal efficiency is metal dependent;

- toxic heavy metals such as Cu, cadmium (Cd), zinc (Zn), nickel (Ni), cobalt (Co) and Pb can be readily removed via SF and SSF wetland systems;
- water level rather than flow pattern in SF system affects the metal removal efficiency; and
- the type of substrate in SSF system seems to influence the removal efficiency of metals.

It is also important to realise that irrespective of the kinds of removal mechanism at work, the wetland systems always have a finite capacity for metal retention though the capacity can be enlarged through choice of substrates, plant species and better engineering design (Lim and Polprasert, 1998). Also cited in their review was the works by Henrot and Wieder (1990), Wieder *et al.* (1990) and Henrot *et al.* (1989) where the dominant removal mechanism in special reference to iron (Fe) seems to be the microbial mediated metal-oxide precipitation.

Because precipitation, adsorption, suspended biofilm (less misleading if known as flocs) and biofilm (the precise term for attached biofilm) co-exist in a wetland system, in order to study only adsorption as well as only the role of the attached biofilm, one need to isolate them from the wetland system. Because live microbes will induce metal-oxide precipitation, the scope has been narrowed down to the role of dehydrated biofilm in the adsorption of Cu (II). Therefore, it makes sense that the objectives of this work are:

- to assess the potential of oil palm shell as an alternative medium;
- to study the another primary removal mechanism, adsorption on substrate; and
- to investigate the effect of the dehydrated biofilm in the adsorption of Cu (II).

1.6.1 Further descriptions on research objectives

The immediate research objectives are summarised below:

1. to prepare potential medium for constructed wetland application from wastes with no chemical modification;
2. to provide first hand brief comparative adsorption capacity data of the oil palm shell and some of the prepared media;
 - although the interest was on Cu (II), other bivalent metals were experimented as well to fill up existing data gaps in reference to media purposely prepared for constructed wetland application. The Cd (II), Zn (II) and Pb (II) were selected as these are the commonly selected model heavy metal of study (Fritioff and Greger, 2006; Cheng *et al.*, 2002b; Scholes *et al.*, 1998; Mungur *et al.*, 1995);
3. to study the growth of *Typha angustifolia* in the presence of different experimental media and different experimental constructed wetland designs;
4. to study the biofilm formation on the oil palm shell in isolated systems;
5. to investigate the effect of biofilm formation in the oil palm shell on its physico-chemistry characteristics;
6. to investigate the effect of various parameters on the adsorption of Cu (II) by the oil palm shell without and with the presence of dehydrated biofilm; and
7. to understand the kinetics of adsorption involved.

In practice, the oil palm shell sample contents some mesocarp fibre (approximately 0.5% v/v) as the mill's separation machinery is not perfect though it exhibit a high level of efficiency. Therefore, the oil palm fibre was experimented in some selected experiments in parallel with the oil palm shell to provide additional supplementary data for future use or reference shall there be a need in future. Other selected media were characterised as well to provide comparisons and evidence to support the thesis discussion.

CHAPTER 2

MATERIALS AND METHODS

2.1 Reagents

All the major chemicals used throughout this research were of A.R. grade and as specified in Table 2.1. Aqueous solutions were prepared by diluting these chemicals with ultrapure water. The ultrapure water was prepared by a series of SG euRO 6A (which produced reversed osmosis water) and SG ultra CLEAR (which eventually produced ultrapure water of 18.18 MΩ) water purifying machines.

Table 2.1: Chemicals used in this study

Name	Formula	Relative molecular mass (g/mol)	Source
Copper nitrate trihydrate	$\text{Cu}(\text{NO}_3)_2 \cdot 3\text{H}_2\text{O}$	241.60	System
Cadmium nitrate tetrahydrate	$\text{Cd}(\text{NO}_3)_2 \cdot 4\text{H}_2\text{O}$	308.47	Fluka
Zinc nitrate-6-hydrate	$\text{Zn}(\text{NO}_3)_2 \cdot 6\text{H}_2\text{O}$	297.48	Riedel-de Haën
Lead (II) nitrate	$\text{Pb}(\text{NO}_3)_2$	331.20	R & M
Nitric acid 65% (w/w)	HNO_3	63.01	Merck
Sodium hydroxide	NaOH	40.00	Merck

The experimental stock solutions of each heavy metal were prepared by diluting exactly 3.80 g $\text{Cu}(\text{NO}_3)_2 \cdot 3\text{H}_2\text{O}$, 2.74 g $\text{Cd}(\text{NO}_3)_2 \cdot 4\text{H}_2\text{O}$, 4.55 g $\text{Zn}(\text{NO}_3)_2 \cdot 6\text{H}_2\text{O}$ and 1.60 g $\text{Pb}(\text{NO}_3)_2$ with ultrapure water to exactly 1 L in order to produce stock solutions of 1000 mg/L of Cu (II), Cd (II), Zn (II) and Pb (II), respectively. These stock solutions were then acidified with three drops of HNO_3 65% (w/w) each, to attain pH 3. It is interesting to note that changes in each heavy metal ion concentration resulted in changes in pH (Figure 2.1). Experiments were normally conducted at $\text{pH } 4.2 \pm 0.2$ which do not require any further pH adjustment for heavy metal ion in the

concentrations range of 40 – 50 mg/L. For experiments that required heavy metal ion concentration out of this range, the respective 1000 mg/L ion stock solution was not been pre-acidified but been diluted to required concentration then only been adjusted to pH 4.2 ± 0.2 with HNO_3 . The purpose of adapting this technique is to avoid or minimise the usage of NaOH.

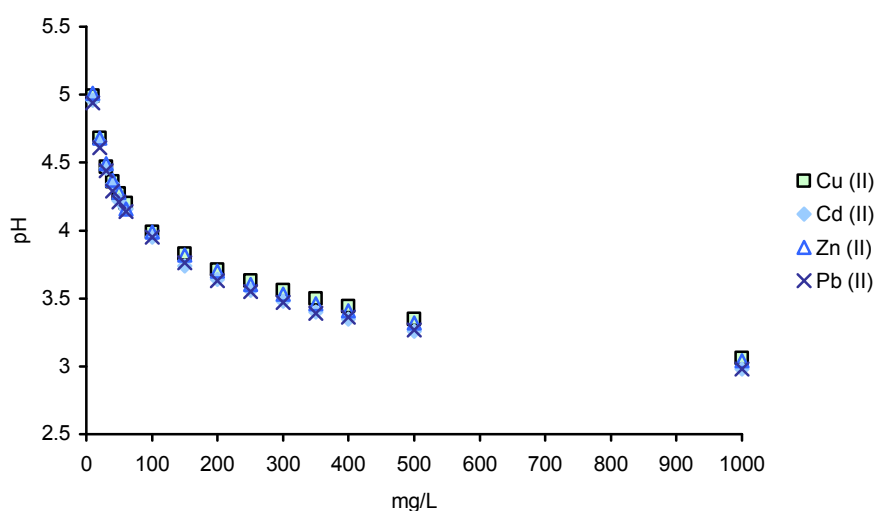


Figure 2.1: The pH of the heavy metal solutions at various concentrations

2.2 Sewage

The sewage used sourced from the university's Desa Aman sewage treatment plant and was filtered through nylon cloth filter to remove suspended particles such as floc, hair *etc.* before being utilised in designated experiments.

2.3 Preparation of Media

All the media used were obtained in the state of Penang where the main campus and the engineering campus of USM are located. In general, these media

were carefully washed with water, dried and processed to required sizes. As a matter of fact, these media were hardly round but granular at their roundest form.

These media, as tabulated in Table 2.2, were categorised into three groups namely, reference media (which serve as low-, carbon based high- and mineral based high-sorptive media), agricultural waste and construction material. Detailed step by step preparations of these media are described in Sections 2.3.1 – 2.3.8 hereafter.

Table 2.2: Categorisation of media

Media	Group
Pea gravel Granular activated carbon Zeolite (Clinoptilolite)	Reference
Oil palm shell Oil palm mesocarp fibre Coconut shell Coconut mesocarp fibre Sugarcane fibre Rice hull	Agricultural waste
Coarse sand Fine sand Wood shave	Construction material

2.3.1 Preparation of pea gravel

Pea gravel was purchased via local supplier. Five random picked samples of 50 g pea gravel soaked overnight in 100 mL HNO_3 10% (w/w) did not give any detection of Cu (II), Cd (II), Zn (II) and Pb (II) when analysed. Therefore, acid washing on this medium was not necessary. The pea gravel was sieved to the size range of $0.5 < \varnothing \leq 1$, $1 < \varnothing \leq 4$ and $4 < \varnothing \leq 5$ mm. Samples were then washed thoroughly, soaked overnight and rinsed with water before being dried at 55 °C for 48 h in the oven. The processed pea gravel was then labelled G.